The Meteoritical Society

Meteoritics & Planetary Science 57, Nr 3, 683–701 (2022)
doi: 10.1111/maps.13789

The distribution of the desert meteorites in China and their classification

Yan FAN[1,2], Shijie LI[2,3]*, Shen LIU[1]*, Hao PENG[4], Guangming SONG[5], and Thomas SMITH[6]

[1]State Key Laboratory of Continental Dynamics and Department of Geology, Northwest University, Xi'an 710069, China
[2]Center for Lunar and Planetary Sciences, Institute of Geochemistry, Chinese Academy of Sciences, Guiyang 550081, China
[3]Chinese Academy of Sciences Center for Excellence in Comparative Planetology, Hefei, China
[4]Xi'an Astronautics Composite Materials Institute, Xian 710025, China
[5]Beijing Institute of Spacecraft Environment Engineering, Beijing 100094, China
[6]State Key Laboratory of Lithospheric Evolution, Institute of Geology and Geophysics, Chinese Academy of Sciences, Beijing 100029, China
*Corresponding author. E-mail: lishijielpsc@mail.gygig.ac.cn; liushen@nwu.edu.cn

(Received 09 June 2021; revision accepted 06 January 2022)

Abstract–In recent years, numerous meteorites have been collected in desert areas in northern and western China. We describe the environment of some deserts in this region, and the petrological and mineralogical characteristics of 49 of the recovered ordinary chondrites. They consist of 14 H chondrites, 33 L chondrites, and 2 LL chondrites. Of the 300 desert meteorites with approved names from deserts in China, there have been 287 ordinary chondrites, six iron meteorites, one CO3 chondrite, one diogenite, one ureilite, one brachinite, one eucrite, and one EL7 chondrite. Forty-two dense meteorite collection areas (DCAs) have been defined, mainly located in northern and western China. The meteorites collected are mainly from the Kumtag DCA, followed by the Alatage Mountain, Loulan Yizhi, Hami, and Lop Nur DCAs. After tentative pairing of the meteorites, we estimate that the ordinary chondrites account for 72% of the desert meteorites collected in China, with 63 H chondrites, 133 L chondrites, and 20 LL chondrites. This dominance of L chondrites contrasts with other deserts, which may result from the insufficient collection or bias in pairing of ordinary chondrites. The mass distribution of meteorites from different DCAs in China is consistent with that from DCAs in Africa. Based on the available information and the meteorite flux model proposed by previous studies, we suggest that the time over which meteorites have been accumulated in the southern Hami DCA might be >10 kyr. Therefore, the southern Hami region is currently the most suitable area for meteorite collection in China.

INTRODUCTION

Meteorites are commonly classified as falls and finds depending on whether they have been observed during their entry into our atmosphere and recovered shortly after they landed (Hutchison, 2007). Most finds come from Antarctica (~64%) and hot deserts (~30%; Drouard et al., 2019). Hot deserts are suitable for the preservation and accumulation of meteorites, mainly due to the arid conditions, the lack of vegetation, and favorable geomorphologic characteristics (Bland et al., 2000; Muñoz et al., 2007; Zolensky et al., 1995). In addition, the advantages of meteorites collected from hot deserts relative to Antarctica include that (1) hot deserts are easier to reach (Muñoz et al., 2007); (2) meteorite searching and collection in hot deserts costs less; (3) unlike Antarctic meteorites, hot desert meteorites are most often found where they fell and can provide statistics about meteorite shower distribution, and the bolide fragmentation processes during the atmospheric entry (e.g., Gnos et al., 2009; Kring et al., 2001; Pourkhorsandi et al., 2019). Therefore, an increasing number of hot deserts have been investigated and sampled; meteorites have been collected and studied from arid areas such as the Australian deserts (Benedix et al., 1999; Bevan & Binns, 1989), the Atacama (Drouard

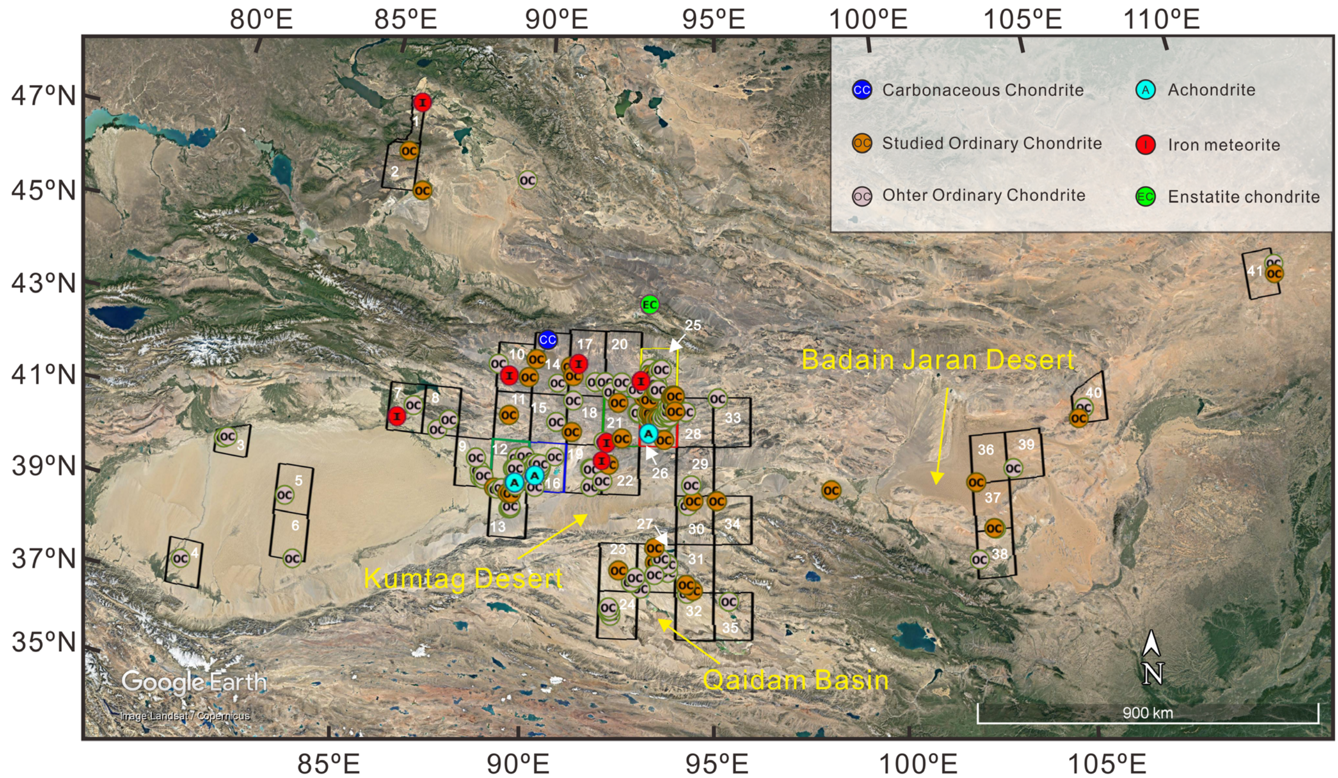

Fig. 1. Map of desert meteorites collected in northern and western China. The rectangle with the thin black borders represents a collection area (see text), which spans a unit of latitude and longitude. The number of collected meteorites less than 10 in dense meteorite collection areas (DCAs) are marked by the black borders, meteorites from 10 to 20 appear in blue, from 20 to 30 in yellow, from 40 to 50 in green, and those with more than 60 stones are in red. The base map is from Google Earth. The numbers figured in white in or around DCAs are linked to the names of DCAs reported in Table 3. (Color figure can be viewed at wileyonlinelibrary.com.)

et al., 2019; Gattacceca et al., 2011; Hutzler et al., 2016; Muñoz et al., 2007), the Sahara (Aboulahris et al., 2019; Bischoff & Geiger, 1995; Ouazaa et al., 2009; Schlüter et al., 2002), the central and southwestern United States (Hutson et al., 2013; Kring et al., 2001; Rubin & Read, 1984; Rubin et al., 2000; Zolensky et al., 1990), the Arabian Peninsula (Al-Kathiri et al., 2005; Gnos et al., 2009; Hezel et al., 2011; Hofmann et al., 2018; Zurfluh et al., 2016), and the Lut Desert (Pourkhorsandi et al., 2019).

There are vast arid areas, mostly stony deserts, distributed in north and western China that are suitable for meteorite collection, such as the Kumtag Desert in the east of Xinjiang Province, the Qaidam Basin in the northeast of Qinghai Province, and the Badain Jaran Desert that spans over three provinces (Inner Mongolia, Ningxia, and Gansu; Fig. 1). However, few desert meteorites have been collected until the discovery of two LL5 ordinary chondrites in Alaer area, Xinjiang, in 2007, which were named Alaer 001 and Alaer 002 (Weisberg et al., 2010). Thereafter, an increasing number of studies on desert meteorites in China were reported (Du et al., 2021; Li & Hsu, 2014; Li et al., 2017, 2021; Zeng et al., 2018). Four meteorite dense collection areas (Xingdi, Argan, Loulan Yizhi, and Lop Nur) in the east of the Taklamakan Desert have been reported by Li and Hsu (2014). Furthermore, Li et al. (2017) identified a chondrite strewn field (Tuya 002-007) in Sanfengshan area, located in the east of Lop Nor, Xinjiang, in which all meteorites were classified as L5 ordinary chondrites, except for Tuya 002, which is an L4. Recently, the Kumtag 016 L5 meteorite shower, the Kumtag H5 meteorite shower, and the Alatage Mountain 001 meteorite shower were identified, and the petrology and cosmic ray exposure ages of samples of these meteorite showers were also reported (Du et al., 2021; Li et al., 2021; Zeng et al., 2018).

Few studies have focused on the desert meteorites in China, so, the collection of desert meteorite in China is to date insufficient as numerous meteorites have not been collected yet. Moreover, meteorite enthusiasts, hunters, and even researchers need reliable guidance to conduct meteorite collection work. Given that there is no report on the detailed distribution of the desert meteorites collected in China, we compile the existing work and combine with new research to summarize the

Table 1. The climate characteristics of the main meteorite collection areas.

	Kumtag		Qaidam		Badain Jaran	
Region	Desert	Stony desert[d]	Basin	Stony desert[d]	Desert	Stony desert[d]
Climate type	Extremely dry continental climate[a]	Warm temperate arid and extremely arid region	Typical continental desert climate[e]	Sub-cold arid climate	Strong continental climate[g]	Temperate arid and extremely arid region
Surface	22,800 km^2		120,000 km^2		50,500 km^2	
Mean annual temperature	10.55 °C[b]	9.8–13.4 °C	2.7 °C[f]	1.1–4.4 °C	7.7–8.2 °C[g]	5–9 °C
Mean annual precipitation	<30 mm[c]	16.4–44.6 mm	<20 mm[f]	17.8–84.6 mm	76.9 mm[h]	<250 mm
Mean annual evaporation		2490.6 mm	3096 mm[f]	2100–3300 mm	>2500 mm[h]	
Dryness degree		16.87–74.36		<10		4–12
Vegetation coverage		<5%		<5%		<10%

[a]From He et al. (2009).
[b]From Lu et al. (2012).
[c]From Dong et al. (2012).
[d]From Shen et al. (2016).
[e]From Qian et al. (2020).
[f]From Zhang and Xuan (1996).
[g]From Yang et al. (2010).
[h]From Zhang et al. (2015).

classification and distribution of all desert meteorites collected in northern and western China. We also estimate the lower limit for the meteorite recovery density and accumulation time in south Hami area based on the larger meteorite showers in this dense meteorite collection area (DCA). Furthermore, we forecast the areas suitable for meteorite recovery, especially for special and rare types of meteorites such as Martian and Lunar meteorites.

DESERT ENVIRONMENT IN CHINA

Due to burial in sand dunes, the chance of finding meteorites is greater in stony desert areas, such as the Kumtag Desert, the Qaidam Basin, and the Badain Jaran Desert in China (Fig. 1). Only a few meteorites (e.g., BG 001-003, Shanshan 001, and Jinta 001) were found in small moving sand dunes in the stony desert around the Badain Jaran Desert and Kumtag Desert, where additional meteorites were collected on the desert surface after these dunes moved. Shen et al. (2016) classified stony deserts in China based on environmental characteristics; specifically, the Kumtag Desert is warm temperate arid and extremely arid, the Qaidam Basin is sub-cold arid and extremely arid, and the Badain Jaran Desert is temperate arid and extremely arid. To date, there have been no reports of the surface ages of these deserts. We briefly introduce the geology and geomorphological characteristics of the main meteorite collection areas (climate characteristics are summarized in Table 1).

Kumtag Desert Area

The Kumtag Desert is located in Xinjiang Province (Fig. 1), and, covering 22,800 km^2, is considered China's sixth largest desert (Dong et al., 2009; Qu et al., 2007; Wei et al., 2007; You-hao et al., 2006). The Kumtag Desert is bounded by the Lop Nur Depression to the northwest; by the eastern branch (Beishan) of the Tianshan Mountains to the north; and by the Altyn Tagh Mountains, which have experienced rapid uplift since the late Pliocene, to the south (Dong et al., 2010, 2012; Li et al., 1979). Gypsum-bearing brown desert soil is developed in the stony desert regions around Kumtag Desert, and the gravels in these regions have black to brown desert varnish (Shen et al., 2016).

Qaidam Basin Area

The Qaidam Basin is the largest intermontane basin in China and is located at the northeastern edge of the Tibetan Plateau, with elevations between 1000 m to more than 6000 m (Liu et al., 1998; Qian et al., 2020).

The basin is bordered by the Kunlun Mountains to the south and to the west, by the Altyn Tagh Mountains to the northwest, by the Qilian Mountains to the northeast, and by the Ela Shan Mountain to the east, covering a total area of 12×10^4 km^2 (Bush et al., 2016; Li et al., 2016; Rieser et al., 2005; Xia et al., 2001). The region has a striking desert landscape with sandy deserts, saline lakes, wind-blown yardangs, and dome dunes, which result from a higher potential evaporation (Li et al., 2016; Qian et al., 2020; Ye et al., 2016). The stony desert in the Qaidam Basin has a gray-brown desert soil and a surface of gravels with black desert varnish (Shen et al., 2016).

Badain Jaran Desert Area

The Badain Jaran Desert is located at the northwest of the Alashan Highland in the western part of Inner Mongolia autonomous region (Fig. 1) (Zhang et al., 2015). The desert is bounded by the Mongolia Altay to the north, by the alluvial/lacustrine plain formed by the Heihe River to the west, by the Qilian Mountains and their branches to the south, and by the Yabulai Mountain and Zongnai Mountain to the east, covering an area of 5.05×10^4 km^2 (Hu & Yang, 2016; Wang et al., 2015; Zhong, 2003). Most of this region has developed gray to brown desert soil, and dark desert varnish occurs on the surface of gravel (Shen et al., 2016).

SAMPLES AND METHODS

Samples

The meteorites studied in this work include 49 ordinary chondrites collected from deserts in Xinjiang, Gansu, Qinghai, and Inner Mongolia (Fig. 1). The meteorites include AM (045-046), Dunlike (007-008), Hami (003-005 and 010-015), Huangtuya (003-004), Kumtag (014, 043-049, 060, 062-064), Lenghu (001 and 004), Loulan Yizhi (046 and 047), Tuanjie (001 and 002), BG 002, Eboliang 005, Erenhot 002, Hoboksar 001, Hongshagang, Hongshijing 001, Muhuren Huduge 001, Niujiaoshan 001, Qiakuertu, Shanshan 001, Turpan 002, Wuerhe, Yangguanzhen 002, YG 001, and YWL 001. Most of the studied ordinary chondrites have brown-black fusion crusts and some are fractured (Fig. 2; Table 2). Additional specimen photographs are available in the supporting information.

Meteorite Classification

Analysis of olivine and low-Ca pyroxene compositions in the studied meteorites was conducted at the Guilin University of Technology. Samples were sliced using a diamond wire saw (STX-603A) and processed as polished thick sections for petrographic and mineralogical investigation. Petrographic observations were conducted on an FEI-Scios field emission scanning electron microscope equipped with energy-dispersive detection spectroscopy at the Institute of Geochemistry, Chinese Academy of Sciences (IGCAS). The instrument was operated at an accelerating voltage of 15–30 kV, a beam current of 0.8–1.6 nA, and a working distance of 7–10 mm. In situ mineral compositions were determined using a JXA 8230 electron probe micro analysis (EPMA), which was operated at an accelerating voltage of 15 kV and an electron beam current of 20 nA. The beam spot diameter ranged from 1 to 10 μm. Natural silicates were used as standards: olivine for Mg and Fe; plagioclase for Si, Al, and Ca; and pyrope garnet for Ti, Cr, and Mn. ZAF-correction was used for data reduction. The detection limits of MgO, Al_2O_3, CaO, and SiO_2 were all 0.01%; Cr_2O_3, FeO, and MnO were 0.02%; NiO, Na_2O, and K_2O were 0.03%; and TiO_2 was 0.05%. The classification of these ordinary chondrites was conducted using the schema of Van Schmus and Wood (1967) and Brearley and Jones (1998). The weathering grade is estimated using the scale proposed by Wlotzka (1993), which is mainly based on the weathering degree of Fe-Ni metal.

Meteorite Search Campaigns

The meteorite search campaigns in deserts in China are all conducted by meteorites hunters by car or by foot, randomly, without a systematic recovery method: at first, a few meteorites were distinguished and collected by our coauthors, geologists, and stone collectors, accidentally in some areas when they worked in the field. Thereafter, meteorite search campaigns were conducted by our team, our coauthors, or other meteorite hunting teams in these areas. We/they searched the areas where meteorites had been collected previously by foot, and then expanded the searching area by car, until another area with meteorites was discovered.

Meteorite Recovery Density

By combining the numbers and information of thoroughly collected meteorites finds in a certain area, one can estimate the meteorite accumulation time based on the meteorite flux, with the hypothesis that the meteorites in the studied area are in saturation; in other words, that there is a dynamic equilibrium between the disappearance of meteorites caused by terrestrial weathering and the fall of meteorites. Because no systematic recovery work has been conducted in China,

Fig. 2. Photographs of some of the desert meteorites studied in this work include (a) Hami 012, (b) Hami 014, (c) Hongshijing 001, (d) BG 002, (e) Kumtag 049, (f) Kumtag 060, (g) Dunlike 007, (h) AM 045, and (i) Hunagtuya 003. More photographs of meteorite samples in this study can be accessed in the supporting information. (Color figure can be viewed at wileyonlinelibrary.com.)

only lower limits for the meteorite recovery density and the accumulation time could be derived in this study.

RESULTS

Classification of the Studied Ordinary Chondrites

The mineral compositions of the 49 studied ordinary chondrites are listed in Table 2 and plotted in Fig. 3. Detailed EPMA analysis data are presented in Table S1 in the supporting information. Some representative backscattered electron (BSE) images of these studied meteorites are presented in Figs. 4 and 5. Additional BSE images are also presented in the supporting information. Based on the petrological characteristics and mineral compositions, the studied ordinary chondrites are classified as one H3 chondrite, six H4 chondrites, seven H5 chondrites, two L3 chondrites, 20

Table 2. List of investigated meteorites, petrographic classification, olivine, and low-Ca pyroxene composition.

Name of meteorites	Classification	Weathering grade	Olivine: Fa (mole%)	PMD	*n* (olivine)	Pyroxene: Fs (mole%)	PMD	Wo (mole%)	*n* (pyroxene)
AM 045	H4	W1	19.3 ± 0.3	1.4	7	16.9 ± 0.6	3.4	0.9 ± 0.4	8
AM 046	L5	W2	24.8 ± 0.4	1.7	8	21.2 ± 0.4	2.0	1.5 ± 0.2	7
Dunlike 007	L6	W2	24.5 ± 0.7	2.8	6	21.1 ± 0.3	1.4	1.4 ± 0.2	5
Dunlike 008	L5	W4	24.3 ± 0.4	1.8	8	19.9 ± 0.4	1.8	4.1 ± 0.4	7
Hami 003	H5	W1	18.7 ± 0.2	1.3	6	17.2 ± 1.3	7.6	1.1 ± 0.2	8
Hami 004	L5	W2	22.8 ± 0.3	1.2	5	19.5 ± 0.4	2.0	0.8 ± 0.5	5
Hami 005	H5	W3	19.7 ± 0.3	1.3	7	17.6 ± 1.1	6.1	1.5 ± 0.2	6
Hami 010	L5	W3	25.5 ± 0.3	1.1	5	21.0 ± 0.9	4.1	1.4 ± 0.2	5
Hami 011	H5	W1	18.7 ± 0.2	1.3	6	16.8 ± 0.5	3.2	1.4 ± 0.1	6
Hami 012	H5	W4	19.1 ± 0.2	0.9	7	17.1 ± 0.3	1.7	1.5 ± 0.3	11
Hami 013	L5	W2	25.5 ± 0.5	1.9	6	20.5 ± 0.4	1.8	1.4 ± 0.1	5
Hami 014	L3	W2	24.3 ± 6.1	25.2	8	13.3 ± 4.6	34.2	1.2 ± 0.9	6
Hami 015	L5	W3	25.2 ± 0.7	2.8	8	21.2 ± 0.6	3.1	1.5 ± 0.2	8
Huangtuya 003	L5	W3	25.1 ± 0.2	0.8	8	21.6 ± 0.5	2.4	1.6 ± 0.2	8
Huangtuya 004	L5	W3	25.7 ± 0.3	1.3	5	21.5 ± 0.3	1.6	1.6 ± 0.1	5
Kumtag 014	L3	W2	22.9 ± 13.5	58.9	45	15.5 ± 9.2	59.5	1.1 ± 1.0	14
Kumtag 043	L6	W1	25.5 ± 0.5	1.9	5	21.8 ± 0.8	3.6	1.5 ± 0.2	5
Kumtag 044	H5	W3	20.0 ± 0.8	3.9	5	16.4 ± 0.3	2.0	1.2 ± 0.5	5
Kumtag 045	L6	W4	25.9 ± 0.5	1.8	10	21.7 ± 0.2	0.9	1.7 ± 0.2	10
Kumtag 046	H5	W4	19.8 ± 0.5	2.4	10	17.6 ± 0.5	2.6	1.4 ± 0.2	10
Kumtag 047	L6	W4	25.1 ± 0.3	1.2	5	20.8 ± 0.2	1.1	1.9 ± 0.1	5
Kumtag 048	L5	W2	24.7 ± 0.4	1.6	7	20.8 ± 0.4	1.9	1.9 ± 0.1	8
Kumtag 049	L6	W4	25.4 ± 0.4	1.5	5	21.7 ± 0.6	2.6	1.6 ± 0.2	6
Kumtag 060	L5	n.a.	24.8 ± 0.3	1.3	6	21.2 ± 0.3	1.3	1.4 ± 0.2	7
Kumtag 062	L6	W4	25.0 ± 0.2	1.0	5	20.7 ± 0.2	0.8	2.0 ± 0.2	4
Kumtag 063	H4	W4	17.4 ± 0.3	1.5	5	14.7 ± 0.3	2.0	0.2 ± 0.0	5
Kumtag 064	L6	W3	25.1 ± 0.3	1.1	5	21.0 ± 0.2	0.9	1.3 ± 0.2	5
Lenghu 001	H4	W2	18.7 ± 0.2	0.9	7	16.7 ± 0.4	2.6	1.3 ± 0.3	5
Lenghu 004	L5	W2	25.4 ± 0.5	2.0	8	21.3 ± 0.5	2.2	1.4 ± 0.3	8
Loulan Yizhi 046	L5	W1	25.2 ± 0.6	2.2	6	20.8 ± 0.5	2.3	1.7 ± 0.2	5
Loulan Yizhi 047	L6	n.a.	24.9 ± 0.2	0.8	5	20.8 ± 0.2	0.9	1.6 ± 0.2	5
Tuanjie 001	H4	W3	17.7 ± 0.3	1.9	5	15.6 ± 0.3	1.6	1.0 ± 0.5	5
Tuanjie 002	L5	W3	25.3 ± 0.4	1.7	10	22.0 ± 0.2	1.0	1.3 ± 0.2	8
BG 002	L5	W2	24.9 ± 0.5	2.0	5	22.0 ± 1.0	4.6	1.4 ± 0.2	5
Eboliang 005	H4	W4	18.9 ± 0.1	0.6	5	17.0 ± 0.4	2.4	1.2 ± 0.2	5
Erenhot 002	L5	W2	25.1 ± 0.6	2.3	5	21.4 ± 0.7	3.3	1.4 ± 0.3	5
Hoboksar 001	L6	W1	26.1 ± 0.2	0.8	5	21.6 ± 0.4	1.8	1.7 ± 0.2	5
Hongshagang	H3	W2	17.9 ± 3.8	21.4	16	13.1 ± 4.0	30.3	1.7 ± 2.6	15
Hongshijing 001	L6	W1	25.6 ± 0.5	1.8	6	21.8 ± 0.6	2.6	1.6 ± 0.2	5
Jinta 001	L5	W2	24.3 ± 0.4	1.5	4	21.1 ± 0.4	1.8	1.5 ± 0.1	4
Muhuren Huduge 001	L5	n.a.	24.1 ± 0.3	1.3	5	20.9 ± 0.6	3.1	1.4 ± 0.1	8
Niujiaoshan 001	H4	W4	19.3 ± 0.3	1.5	3	17.1 ± 0.3	1.5	1.5 ± 0.1	3
Qiakuertu	H5	W4	18.6 ± 0.1	0.4	5	16.5 ± 0.2	1.1	1.2 ± 0.2	5
Shanshan 001	LL5	W1	30.1 ± 0.7	2.3	9	24.9 ± 0.8	3.0	1.9 ± 0.1	7
Turpan 002	LL5	W3	29.1 ± 0.6	2.1	10	23.6 ± 0.3	1.4	1.7 ± 0.2	9
Wuerhe	L5	W1	25.0 ± 0.6	2.3	5	21.2 ± 0.3	1.3	1.4 ± 0.2	5
Yangguanzhen 002	L6	W3	25.4 ± 0.6	2.3	5	20.0 ± 0.5	2.4	1.7 ± 0.2	10
YG 001	L5	W3	25.3 ± 0.5	2.1	6	21.9 ± 0.7	3.0	1.2 ± 0.2	5
YWL 001	L5	W1	24.5 ± 0.3	1.2	5	20.4 ± 0.2	1.1	1.5 ± 0.1	5

Errors for Fa and Fs are 1σ standard deviations. PMD = percent mean deviation; n.a. = not analyzed. The full datasets of mineral chemistry can be accessed in Table S1.

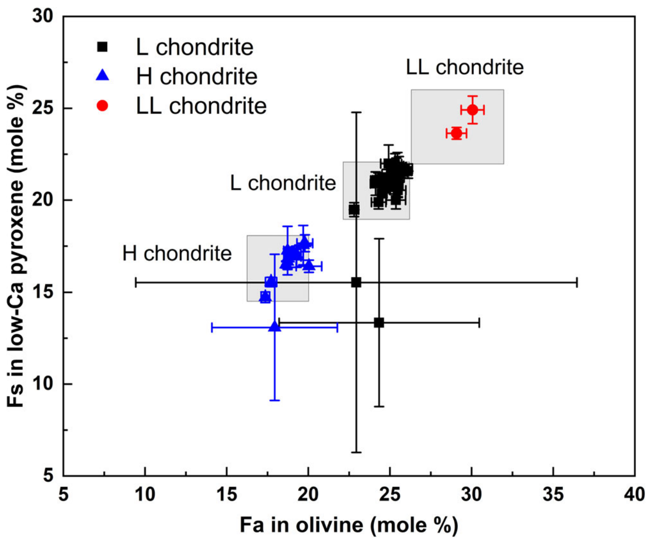

Fig. 3. Olivine fayalite (Fa) versus low-Ca pyroxene ferrosilite (Fs) contents for the studied desert meteorites (modified from Brearley & Jones, 1998). Error bars reflect 1σ standard deviation. The outlier samples with the large error bars are to Hami 014 (L3; right-hand one), Kumtag 014 (L3; top one) and Hongshagang (H3). (Color figure can be viewed at wileyonlinelibrary.com.)

L5 chondrites, 11 L6 chondrites, and two LL5 chondrites (Table 2). More information (such as coordinates and recovered mass) is presented in Table S2 in the supporting information. The estimated weathering grades of the studied ordinary chondrites are also listed in Table 2; in summary, they consist of nine W1 meteorites, 13 W2 meteorites, 13 W3 meteorites, and 11 W4 meteorites. Specifically, Loulan Yizhi 046 (Fig. 4e) is a melt breccia, where melt region I is mainly composed of olivine with normal and reverse zoning (normal with Mg-rich in core and Fe-rich at rim), consistent with the incomplete melting and rapid crystallization typical of shock processes. Regions II and III are completely melted and are characterized by tiny euhedral to subhedral olivine grains, and skeletal olivine crystals embedded in the mesostasis (Figs. 4e and 4f). In addition, SiO_2-rich components (SRCs) and alkali-feldspar are detected in Hami 014 and Kumtag 014 (e.g., Figs. 5e and 5g). SRCs are formed in the solar nebula by fractional condensation, whereas alkali-feldspars with a primary igneous texture are formed from melt having the bulk composition of the host chondrules (Hezel et al., 2006; Lewis & Jones, 2019).

Information about other desert meteorites collected in China was collected from the Meteoritical Bulletin Database (https://www.lpi.usra.edu/meteor/metbull.php) and is summarized in Table 3. The number of ordinary chondrites (after tentative pairing) of each type from different deserts and some DCAs is presented in Table 4 and is plotted in Fig. 6.

Mass Distribution

The desert meteorites collected from some DCAs in China were binned in mass categories (0.1–1; 1–10; 10–100; 100–1000; 1000–10,000; 10,000–100,000; 100,000–1,000,000 g) to compare the mass distribution between different DCAs. The percentages of each range were calculated and plotted (Table 5; Fig. 7).

Meteorite Shower and Meteorite Pairing

The tentative pairing of the ordinary chondrites collected in desert areas in China is estimated using the petrology type, the weathering grade, the mineral composition, the already distinguished or reported meteorite shower, the spatial distance between individual find locations, and the shape of meteorites. Four meteorite showers in desert areas in China have been reported, including AM 001-042 (L5, S5, W2) meteorite shower, with total collected mass ~200 kg (Li et al., 2021); Kumtag (H5) meteorite shower with total collected mass ~180 kg (Du et al., 2021); Kumtag 016 (L5, S4, W2-3) meteorite shower (including meteorites Kumtag 015-020, 022-031, and 033-038) with total collected mass ~500 kg (Zeng et al., 2018); and Tuya 003-007 (L5, S2, W3) meteorite shower with total collected mass ~160 kg (Li et al., 2017). Therefore, meteorites AM 001-042; Kumtag 015-020, 022-031, and 033-038; and Tuya 003-007 are paired. The mineral compositions and the find location of AM 047 are consistent with samples from the AM 001-042 meteorite shower, indicating AM 047 (50 kg) should also be paired with AM 001-042. Loulan Yizhi 048 and 049 should be paired with Loulan Yizhi 047 because they have consistent mineral compositions, petrological types, weathering grades, magnetic susceptibilities, and find location. In addition, a few of the collected meteorites, having large masses and numerous pieces, likely represent a single meteorite shower, including Kumtag 047 (~90 kg), Kumtag 062 (~200 kg), Dunlike 007 (30 kg), Dunlike 008 (10 kg), Loulan Yizhi 047 (190 kg), Eboliang 005 (~25 kg), YWL 001 (~140 kg), Erenhot 002 (~38 kg), Hoboksar (15 kg), Lop Nur 015 (29 kg), and Wuerhe (~6 kg). Furthermore, the total mass of meteorites collected in Bayin Gobi DCAs is larger than 300 kg (each single meteorite being larger than 1 kg). Three meteorites with approved names were collected including L5 chondrites (BG 001 and 002) and one L6 chondrite (BG 003); both BG 001 and BG 002 are thought to be paired based on their similar petrological types and shapes. Although BG 003 was classified as a L6 chondrite recently, it is likely the product of a single meteorite shower, together with BG 001 and BG 002, because all the meteorites collected in this area have similar surface features and similar

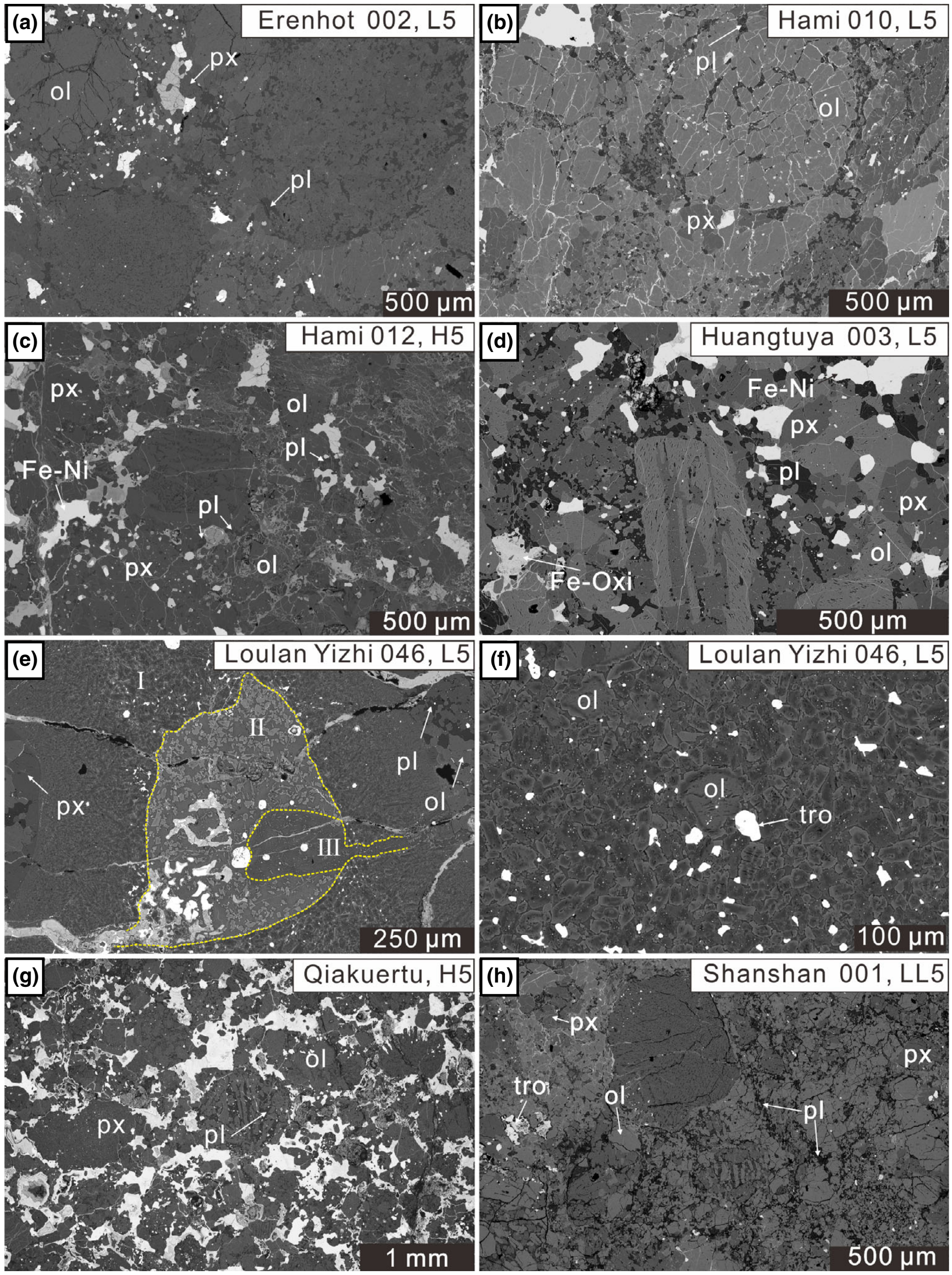

Fig. 4. Backscattered electron (BSE) images of representative 5-type chondrite.a, b, d, f) L5 chondrite (Erenhot 002, Hami 010, Huangtuya 003, and Loulan Yizhi 046, respectively).c, e, g) H5 chondrite (Hami 012, Kumtag 044, and Qiakuertu, respectively).h) LL5 chondrite (Shanshan 001). ol = olivine, px = pyroxene, pl = plagioclase, tro = troilite, Fe-Ni = Fe-Ni metal; Fe-Oxi = Fe-oxide/oxyhydroxide. Additional BSE images of meteorite samples in this study can be accessed in the supporting information. (Color figure can be viewed at wileyonlinelibrary.com.)

rectangular shapes with near ~90° angles (according to pictures from the Meteoritical Bulletin Database).

Meteorite Recovery Density

Considering that the meteorites found either in areas with light-colored granitic rock and soil, or in meteorite showers, are easier to be recognized than single and small meteorites, three areas are defined to estimate the meteorite recovery density, which includes two light-colored granitic areas (about 44.7 km^2 for area A and about 151 km^2 for area B) in the southern Gobi area of Hami, and one area (area C) with five meteorite showers identified (Fig. 8). For area C, only

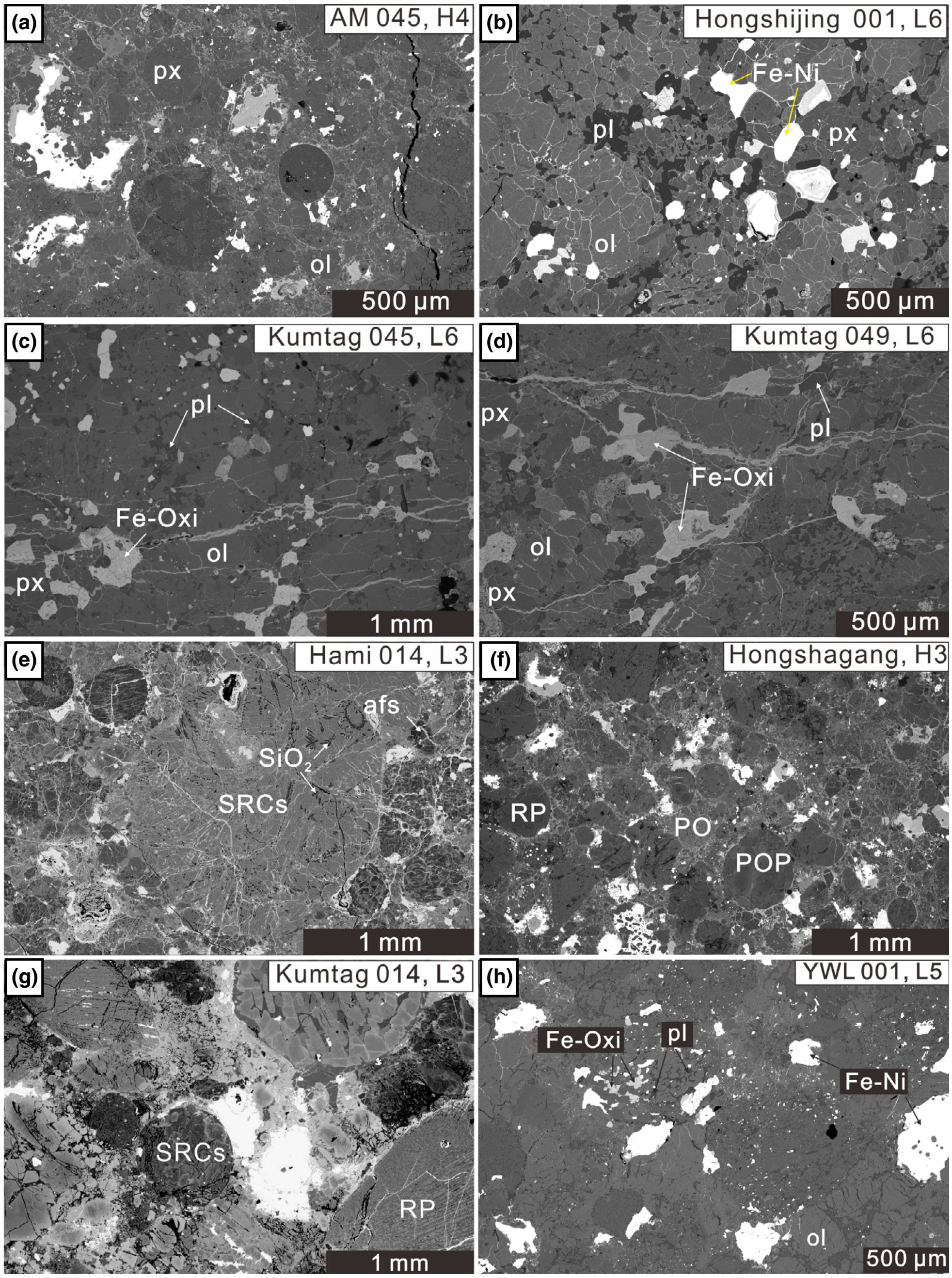

Fig. 5. a) BSE images of representative H4 chondrite (AM 045). b–d) BSE images of representative L6 chondrite (Hongshijing 001, Kumtag 045, and Kumtag 049, respectively). e, g) BSE images of L3 chondrite (Hami 014 and Kumtag 014, respectively). f) BSE images of H3 chondrite (Hongshagang). h) BSE images of L5 chondrites (YWL 001). ol = olivine; px = pyroxene; pl = plagioclase; afs = alkali feldspar; tro = troilite; Fe-Ni = Fe-Ni metal; Fe-Oxi = Fe-oxide/oxyhydroxide; SRCs = SiO_2-rich components. The chondrule type includes porphyritic olivine chondrule (PO), radial pyroxene chondrule (RP), and porphyritic olivine-pyroxene chondrule (POP). More BSE images of meteorite samples in this study can be accessed in the supporting information.

samples from meteorite showers were used to estimate meteorite recovery density and accumulation time. The delineation of area C is primarily based on the area searched and on the consensus that this area is rich in meteorite showers. Two estimated meteorite flux models proposed by Halliday et al. (1989) and Evatt et al. (2020) are used to estimate the meteorite accumulation time. The meteorite collections, meteorite fluxes with different masses, meteorite recovery density, and meteorite accumulation time of collected meteorites in

Table 3. The type statistics of desert meteorites in each collection area in China.

DCA names	Meteorites H	L	LL	CO3	Diogenite	Iron meteorite	Ureilite	Brachinite	EL7 chondrite	Eucrite	Total number of meteorites	Meteorite shower	DCA serial number
Kumtag	7	54	2					1			64	4	26
Alatage Mountain	2	44				1					47	1	21
Loulan Yizhi	15	26	4				1				46	1	12
Hami	8	11	1			1					21	0	25
Lop Nur	6	8			1						15	1	16
Dunlike	3	5	1								9	2	13
Xinjiang*	1	6	1								8	0	
Ganq		7									7	0	24
Tuya	1	6				1					8	1	19
Lenghu	3	4									7	0	27
Argan	2	3									5	0	9
Eboliang	1	4									5	1	23
Alaer		0	4								4	0	3
Huangtuya	1	2				1					4	0	17
Bayin Gobi		3									3	1	40
Turpan		1	1			1					3	0	10
Wubao	1	1	2								4	0	20
Erenhot	1	1									2	1	41
Hongshagang	1	1									2	0	37
Hongshijing		1	1								2	0	22
Korla	1					1					2	0	7
Shanshan		1	1	1							3	0	14
Tuanjie	1	1									2	0	31
Xingdi	1	1									2	0	8
Yangguanzhen		1	1								2	0	30
Yuweilinag	1	1									2	1	18
Baqiangzi*									1		1	0	
Da Qaidam		1									1	0	35
Dunhuang		1									1	0	29
Hoboksar		1									1	1	2
Jeminay						1					1	0	1
Jinchang	1										1	0	38
Jinta 001*		1									1	0	
Liuyuan		1									1	0	33
Mount Yirtkuq Bulak	1										1	0	15
Muhuren Huduge		1									1	0	36
Nanbaxian		1									1	0	32
Niujiaoshan	1										1	0	11
Pakepake		1									1	0	6

Table 3. *Continued*. The type statistics of desert meteorites in each collection area in China.

DCA names	Meteorites H	L	LL	CO3	Diogenite	Iron meteorite	Ureilite	Brachinite	EL7 chondrite	Eucrite	Total number of meteorites	Meteorite shower	DCA serial number
Qiakuertu*	1										1	0	
Qira	1										1	0	4
Tamusubulage			1								1	0	39
Tazhong	1										1	0	5
Weiya		1									1	0	28
Wuerhe*		1									1	1	
Yiwu 001*										1	1	0	
Yibaisi Gobi		1									1	0	34
Total	63	204	20	1	1	7	1	1	1	1	300	16	

Areas with the symbol "*" refer to the collection areas which have not been defined as DCAs. Areas without the symbol "*" refer to the DCAs. These meteorites were not paired. The DCA serial numbers are linked to Fig. 1.

Table 4. The numbers of ordinary chondrites of each type (H, L, and LL) from different deserts and some typical DCAs in China.

Areas	Ordinary chondrite type H	L	LL	H/L
Kumtag DCA	7	33	2	0.21
Alatage Mountain DCA	2	2	0	1.00
Loulan Yizhi DCA	15	24	4	0.63
Hami DCA	8	11	1	0.73
Lop Nur DCA	6	8	0	0.75
Kumtag Desert	51	101	14	0.50
Qaidam Basin	5	18	0	0.28
Badain Jaran Desert	2	3	1	0.67
China	63	133	20	0.47

The meteorites adopted for statistical analyses in this table have been tentatively paired.

these areas are presented in Table 6. The meteorite flux has been corrected for the latitude effect according to the latitude model proposed by Evatt et al. (2020).

DISCUSSION

Meteorites Collected in Different Desert Areas in China

DCAs are regions where numerous meteorites are recovered (e.g., Gattacceca et al., 2011; Hutson et al., 2013; Hutzler et al., 2016; Ouazaa et al., 2009; Pourkhorsandi et al., 2017). To date, 42 DCAs have been defined in China by the Meteoritical Society, which are mainly located in/around Kumtag Desert and Qaidam Desert, with five DCAs located in/around Badain Jaran Desert; Erenhot located in the Kubuqi Desert; Alaer and Qira located at the north and southwest margin of the Taklimakan Desert; and Hoboksar, Jeminay, and Wuerhe located at the northwest margin of the Gurbantunggut Desert (Fig. 1). After tentative pairing of the meteorites, the DCAs with more than 10 collected meteorites include Kumtag, Loulan Yizhi, Hami, and Lop Nur. The mass of desert meteorites from China is mainly concentrated between 10 and 1000 g with a peak between 100 and 1000 g, which is consistent with that from Africa (peak between 100 and 1000 g), but inconsistent with that from both Australia (peak between 10 and 100 g) and Antarctica (peak at <10 g) (Ouknine et al., 2019). The mass distribution of collected meteorites from Loulan Yizhi and Lop Nur shows a maximum within 10–100 g, while those from Kumtag and Hami are mainly distributed in the range 100–1000 g. The mass distributions of these DCAs correspond to those of DCAs from other deserts such as Tieret, Bir Zar, UAE, San Juan, Dhofar, and Acfer (Aboulahris et al., 2019). The difference in the mass distribution of collected meteorites from China, Africa, Australia, and Antarctica is mainly explained by the differences in surface features and collection methods (Ouknine et al., 2019). For instance, smaller meteorites are easier to be recognized with the generally white to blue background in Antarctica in contrast to the background of hot desert (Zolensky et al., 2006).

So far, 300 desert meteorites with approved names have been collected in China's deserts, including 287 ordinary chondrites, seven iron meteorites, one CO3 chondrite, one diogenite, one ureilite, one brachinite, one eucrite, and one EL7 chondrite. Unfortunately, there are still numerous unnamed desert meteorites in the possession of hunters, who are sometimes not willing to provide these meteorites. After tentative pairing of the meteorites, the ordinary chondrites recovered in China account for 72% of the total desert meteorites found in China, with 63 H chondrites, 133 L chondrites, and 20 LL chondrites. Specifically, the numbers of ordinary chondrites of each type (H, L, LL) from different deserts are as follows: Kumtag Desert (51H/101L/14LL), Qaidam Basin (5H/18L), and Badain Jaran Desert (2H/3L/1LL). In some typical DCAs of the Kumtag Desert, the numbers of ordinary chondrites of each type are as follows: Kumtag (7H/33L/2LL), Alatage Mountain (2H/3L), Loulan Yizhi (15H/24L/4LL), Hami (8H/11L/1LL), and Lop Nur (6H/8L). These ordinary chondrites type ratios are all characterized by a dominance of L chondrites, followed by H, and then LL chondrites, which is the opposite of DCAs from Sahara, Algeria, and Libya (Aboulahris et al., 2019; Ouknine et al., 2019). The dominance of L chondrites in the deserts of China may result from the lack of a systematic recovery method for the ordinary chondrite collection or might be caused by an insufficient pairing due to the lack of accurate information about the ordinary chondrites other than our samples studied in this paper.

The Most Suitable Area for Meteorite Collection in China

The meteorite flux is generally estimated by short-duration fireball monitoring networks (Bland et al., 2012; Halliday et al., 1989, 1996; Howie et al., 2017) or ground-based meteorite search campaigns in deserts (Bland et al., 1996; Drouard et al., 2019; Evatt et al., 2020; Gattacceca et al., 2011; Hutzler et al., 2016; Hughes, 1992). Both of the meteorite flux models used in this study belong to the second approach, which estimates the total mass of meteorites that reached the ground for each single event. Considering the absolute number of search campaigns and considering that the

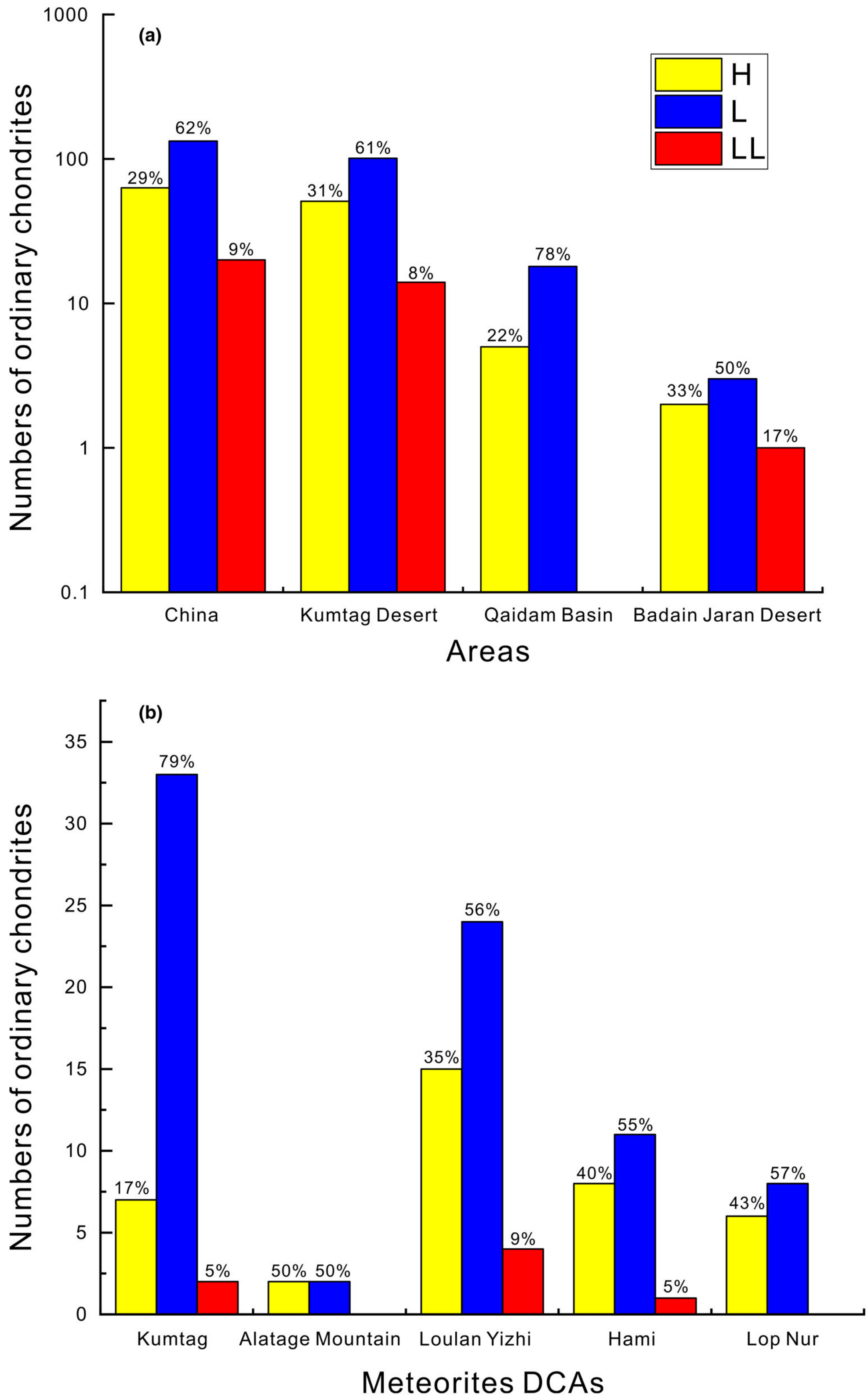

Fig. 6. a) Number of ordinary chondrites H, L, LL in different hot deserts and China after tentative pairings. b) Number of ordinary chondrites H, L, and LL in different dense meteorite collection areas (DCAs) in and around Kumtag Desert after tentative pairings. Data extracted from that available in the Meteoritical Bulletin Database. (Color figure can be viewed at wileyonlinelibrary.com.)

Table 5. Total number and percentage of collected meteorite mass (g) from China, and some DCAs.

Areas	Total number	Percentage of meteorite mass (g)						
		0.1–1	1–10	10–10^2	10^2–10^3	10^3–10^4	10^4–10^5	10^5–10^6
China	229	0	7	29	30	21	10	3
Kumtag DCA	43	0	2	14	44	26	7	7
Hami DCA	21	0	0	24	52	10	14	0
Loulan Yizhi DCA	44	0	20	45	20	11	0	2
Lop Nur DCA	15	0	0	60	27	7	7	0

Meteorites were binned on seven mass intervals (0.1–1; 1–10; 10–100; 100–1000; 1000–10,000; 10,000–100,000; 100,000–1,000,000 g). The meteorites adopted for statistical analyses in this table have been tentatively paired.

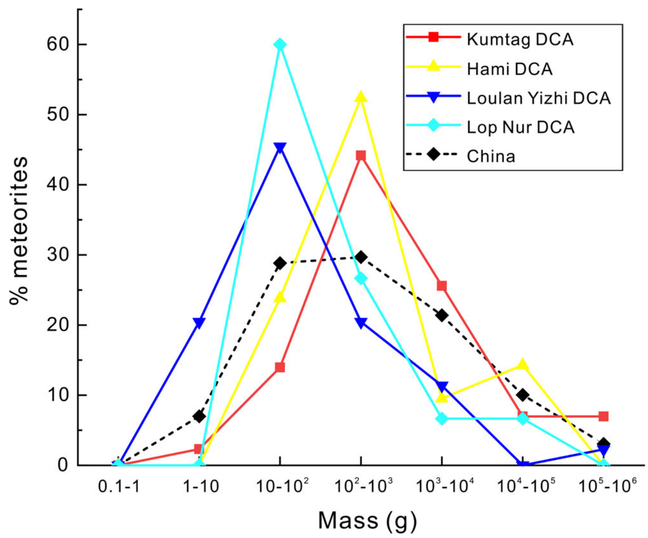

Fig. 7. Mass distribution of meteorites collected from China and some dense meteorite collection areas (DCAs) in hot deserts after tentative pairings. Data extracted from that available in the Meteoritical Bulletin Database. (Color figure can be viewed at wileyonlinelibrary.com.)

number of meteorite samples collected during these campaigns in hot deserts is much lower than that in Antarctica, we prefer using the meteorite flux estimate approach proposed by Evatt et al. (2020). Based on the fluxes of 9.3 meteorites km^{-2} Myr^{-1} (>411 g) and 37.3 meteorites km^{-2} Myr^{-1} (>34 g) for areas A and B, respectively (Fig. 8), the calculated meteorite accumulation time is ~9.6 kyr for area A but only ~0.9 kyr for area B (Table 6). The extremely low accumulation time for area B may be explained by the deficit of meteorites with small masses combined with the use of meteorite flux with low total meteorites collected mass. For area C, in which five meteorite showers were determined and the minimum total collected mass among them is 90 kg (Fig. 6c), the accumulation time is ~10 kyr, which is estimated considering a meteorite flux of 0.24 meteorites km^{-2} Myr^{-1} (>90 kg) from Halliday et al. (1989); note that the meteorite flux was also corrected for the latitude effect according to the latitude model proposed by Evatt et al. (2020) (Table 6). Previous studies suggest that small meteorites could be collected effectively by systematic search by foot; however, searching randomly by foot or vehicle favors bigger finds (Aboulahris et al., 2019). Considering the lack of systematic search in these areas (A, B, and C), we suggest that the error on the meteorite accumulation time estimated from area C should be lower than that from areas A and B. Therefore, we preferred 10 kyr as the appropriate estimation of the lower limit of meteorite accumulation time for the southern Hami area. Future accurate terrestrial age measurements of meteorites from the meteorite shower could provide further constraints on the flux of large meteorites (especially for the total collected mass larger than 10 kg).

The terrestrial ages of most ordinary chondrites from hot deserts range from almost zero to 40 kyr (with a peak around 20 kyr) (Gattacceca et al., 2011; Pourkhorsandi et al., 2017; Zurfluh et al., 2016) and rarely exceed 50 kyr (Jull, 2006). However, Drouard et al. (2019) found that the terrestrial age for desert stony meteorites is up to 710 kyr in samples from the El Médano area, in the Atacama Desert, Chile. The climate of Kumtag stony desert is arid with low mean annual precipitation (16.4–44.6 mm), which is similar to that of Lut Desert where >200 meteorites have been collected with terrestrial ages ranging from 10 to 30 kyr (Pourkhorsandi et al., 2019). Therefore, the southern Hami area may have a surface age similar to that of Lut Desert and preserve numerous meteorites in the estimated accumulation time interval for area C (10 kyr). The lower estimated accumulation time and meteorite recovery density in area B may result from the limited meteorite research campaigns; thus, a systematic search for meteorites in this area is necessary.

Considering that meteorite hunters, meteorite enthusiasts, and researchers are fascinated by rare types of meteorites such as Lunar and Martian meteorites, we are able to give an estimation of their accumulation on the hot deserts of China based on our study. It has been suggested that achondrites can survive longer than chondrites based on observations from Antarctica (Jull

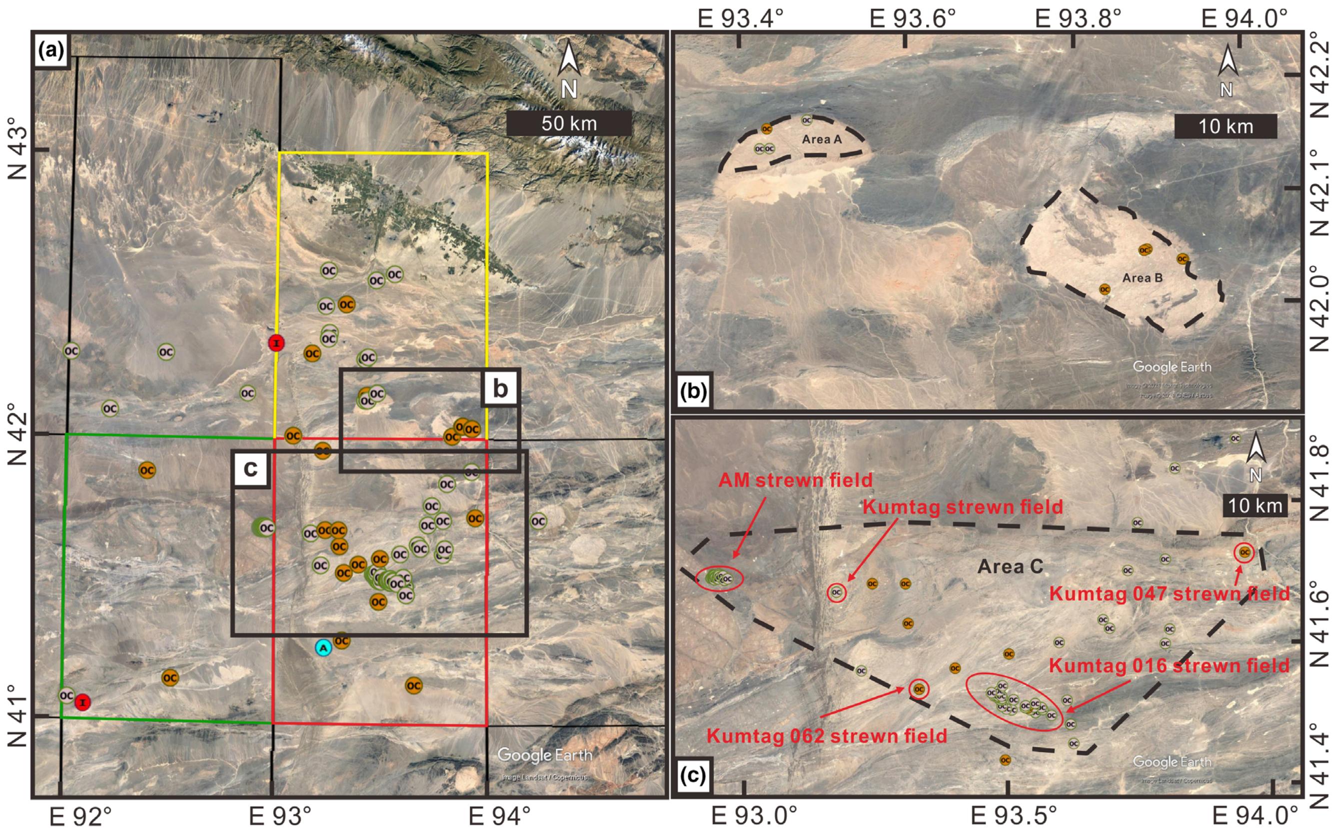

Fig. 8. The distribution of meteorites collected in Hami, Kumtag, and Alatage Mountain. a) A granite area with the acreage of about 44.7 km^2. b) A granite area with the acreage of about 151 km^2. c) A designate area with the acreage of about 2106 km^2. The base map is from Google Earth. The colors of collection area borders correspond to Fig. 1. (Color figure can be viewed at wileyonlinelibrary.com.)

Table 6. The acreage, meteorite mass, meteorite recovery density, and meteorite accumulation time for areas A, B, and C.

Area	Granite area A	Granite area B	Area C	Area C	Area C
S (km^2)	44.7	151	2106	2106	2106
n	4	5	5	1*	1$^{\#}$
m_T (g)	411	34	90,000	1000	1000
Meteorite recovery density ([10^6 km^2]$^{-1}$)	89,485	33,113	2374	475	475
Average latitude	42.14°N	42.03°N	41.55°N	41.55°N	41.55°N
N^a (yr^{-1} [10^6 km^2]$^{-1}$)	14.5	49.3	0.2	0.2	0.04
N^b (yr^{-1} [10^6 km^2]$^{-1}$)	9.3	37.3	n.g.	0.1	0.02
Accumulation time^a (year)	6167	672	10,081	2455	12,274
Accumulation time^b (year)	9657	887	n.g.	4645	23,227

S refers to the acreage of area; n is the number of the collected meteorite after excluding the pairing with the total mass equal to or larger than m_T. N^a and N^b refer to the meteorite flux derived from Halliday et al. (1989) and Evatt et al. (2020), respectively. The use of cutoff masses of 411 and 34 g mainly depends on the minimum total collected mass of each meteorite collected in these areas. Meteorite recovery density and accumulation time refer to the lower limits of the meteorite recovery density and accumulation, respectively. n.g. = not given. "*" and "#" refer to the assumed Lunar meteorite and Martian meteorites with a minimum mass of 1 kg, respectively.

et al., 1998). In particular, relative lack of metal and the compact nature of most Lunar and Martian meteorites means that they can survive longer, for example, those from Dhofar or Oman, have exposure ages of 500 and 350 kyr, respectively. Few ordinary chondrites from Dhofar or Oman can survive longer than ~40–50 kyr under the prevalent environmental conditions (Nishiizumi et al., 2002; Zurfluh et al., 2016). Therefore, based on the estimated accumulation time for ordinary chondrites in area C (Fig. 8), it is possible that Lunar or Martian meteorites falling within the last 100 ka could be preserved. Nazarov et al. (2004) suggested that the annual flux of Lunar meteorites in the mass interval from 10 g to 1 kg to the entire Earth's surface should likely range from tens to few hundreds of kilograms, that is, a few percent of the total meteorite flux. When assuming that the Lunar meteorite flux accounts for 2% of the total meteorite flux, the southern Hami area C should witness the fall of one Lunar meteorite (with a total collected mass no less than 1 kg) every 4.6 kyr (Table 6). Furthermore, based on the Martian meteorites flux ($\sim 4 \times 10^2$ kg yr^{-1}), which corresponds to ~4‰ of the total meteorite flux (Hutchison, 2007; Vickery & Melosh, 1987), we can deduce that southern Hami area C should witness the fall of one Martian meteorite (with a total collected mass no less than 1 kg) every 23.2 kyr (Table 6). Therefore, the meteorite shower enriched area in southern Hami is the most suitable area for meteorite collection in China, and especially for the recovery of Lunar and Martian meteorites.

CONCLUSION

1. In this work, the 49 studied ordinary chondrites collected in desert areas in northern and western China are classified as 33 L chondrites, 14 H chondrites, and 2 LL chondrites.
2. Forty-two DCAs have been defined in China by the Meteoritical Society. There are 300 meteorites with approved names which were collected in China deserts, which mainly consist of 287 ordinary chondrites and six iron meteorites. In addition, a few rare meteorites were also recovered, including one CO3 chondrite (Shanshan 002), one diogenite (Lop Nur 011), one ureilite (Loulan Yizhi 034), one brachinite (Kumtag 061), one eucrite (Yiwu 001) and one EL7 chondrite (Baqiangzi). These meteorites are mainly from Kumtag DCA, followed by Alatage Mountain, Loulan Yizhi, Hami, and Lop Nur DCAs.
3. After tentative pairing, the ordinary chondrites account for 72% of the desert meteorites collected in China. L chondrites are the dominant group of ordinary chondrites in China and in DCAs therein. The numbers of each type of ordinary chondrites collected from some DCAs are as follows: Kumtag (7H/33L/2LL), Alatage Mountain (2H/2L), Loulan Yizhi (15H/24L/4LL), Hami (8H/11L/1LL), and Lop Nur (6H/8L). Among ordinary chondrites, the dominance of L chondrites in China may result from the insufficient collection or bias in pairing of ordinary chondrites.
4. The peak in the mass distribution of desert meteorites collected from China, Kumtag DCA and Hami DCA, is between 100 and 1000 g, while that for the Loulan Yizhi DCA and Lop Nur DCA is between 10 and 100 g.
5. The meteorite shower-enriched area in southern Hami DCA is the most suitable area for meteorite collection in China, with an accumulation time of >10 kyr. This area may have the potential to preserve special/rare type of meteorites such as Lunar and Martian meteorites.

Acknowledgments—This work was supported by the Strategic Priority Research Program of the Chinese Academy of Science, Grant No. XDB41000000, the Chinese Academy of Sciences "Light of West China" Program (Shijie Li, 2019), and the Civil Aerospace Preresearch Project (D020304). We thank all meteorite hunters who provided desert meteorites and useful information related to this study. And we thank Professor Weibiao Hsu from the Purple Mountain Observatory, Chinese Academy of Sciences for providing some desert meteorites. We thank the FIB laboratory team at IGCAS for the SEM observation and BSE image. We thank Dr. Lanfang Xie from the Guilin University of Technology for her assistance in the EMPA laboratory. We would like to express our gratitude to Dr. Katherine Joy for editing the manuscript and for providing precious comments. We also thank Dr. Andy Tomkins and Dr. Jérôme Gattacceca for their valuable comments that greatly improved this paper, and Dr. A. J. Timothy Jull for his help as editor.

Data Availability Statement—The data that support the findings of this study are available in the supplementary material of this article.

Editorial Handling—Dr. Katherine Joy

REFERENCES

Aboulahris, M., Chennaoui, A. H., Rochette, P., Gattacceca, J., Jull, A. T., Laridhi, O. N., Folco, L., and Buhl, S. 2019. Characteristics of the Sahara As a Meteorite Recovery Surface. *Meteoritics & Planetary Science* 54: 2908–28.

Al-Kathiri, A., Hofmann, B. A., Jull, A. J. T., and Gnos, E. 2005. Weathering of Meteorites from Oman: Correlation of Chemical and Mineralogical Weathering Proxies with ^{14}C Terrestrial Ages and the Influence of Soil Chemistry. *Meteoritics & Planetary Science* 40: 1215–39.

Benedix, G. K., Keil, K., and Murakami, J. Y. 1999. Classification of Ten New Nullarbor Region Meteorites. *Meteoritics & Planetary Science* 34: 813–5.

Bevan, A. W. R., and Binns, R. 1989. Meteorites from the Nullarbor Region, Western Australia: I. A Review of Past Recoveries and a Procedure for Naming New Finds. *Meteoritics* 24: 127–33.
Bischoff, A., and Geiger, T. 1995. Meteorites from the Sahara: Find Locations, Shock Classifications, Degree of Weathering and Pairing. *Meteoritics & Planetary Science* 30: 113–22.
Bland, P. A., Bevan, A. W. R., and Jull, A. J. T. 2000. Ancient Meteorite Finds and the Earth's Surface Environment. *Quaternary Research* 53: 131–42.
Bland, P., Smith, T., Jull, A., Berry, F., Bevan, A., Cloudt, S., and Pillinger, C. 1996. The Flux of Meteorites to the Earth Over the Last 50 000 Years. *Monthly Notices of the Royal Astronomical Society* 283: 551–65.
Bland, P. A., Spurný, P., Bevan, A. R., Howard, K. T., Towner, M. C., Benedix, G. K., Greenwood, R. C. et al. 2012. The Australian Desert Fireball Network: A New Era for Planetary Science. *Australian Journal of Earth Sciences* 59: 177–87.
Brearley, A. J., and Jones, R. H. 1998. Chondritic Meteorites. In *Planetary Materials*, edited by J. J. Papike, 3-1–3-398. Reviews in Mineralogy, Vol. 36. Washington, D.C.: Mineralogical Society of America.
Bush, M. A., Saylor, J. E., Horton, B. K., and Nie, J. 2016. Growth of the Qaidam Basin During Cenozoic Exhumation in the Northern Tibetan Plateau: Inferences from Depositional Patterns and Multiproxy Detrital Provenance Signatures. *Lithosphere* 8: 58–82.
Dong, Z., Lv, P., Lu, J., Qian, G., Zhang, Z., and Luo, W. 2012. Geomorphology and Origin of Yardangs in the Kumtagh Desert, Northwest China. *Geomorphology* 139–140: 145–54.
Dong, Z., Qu, J., Lu, J., Qian, G., Luo, W., Wang, X., and Zhou, Q. 2009. *Geomorphic Map of the Kumtagh Desert*. Beijing: Science Press.
Dong, Z., Wei, Z., Qian, G., Zhang, Z., Luo, W., and Hu, G. 2010. "Raked" Linear Dunes in the Kumtagh Desert, China. *Geomorphology* 123: 122–8.
Drouard, A., Gattacceca, J., Hutzler, A., Rochette, P., Braucher, R., Bourlès, D., Team, A., Gounelle, M., Morbidelli, A., and Debaille, V. 2019. The Meteorite Flux of the Past 2 my Recorded in the Atacama Desert. *Geology* 47: 673–6.
Du, K. E., Li, S., Leya, I., Smith, T., Zhang, D., and Wang, P. 2021. The Kumtag Meteorite Strewn Field. *Advances in Space Research* 67: 4089–98.
Evatt, G., Smedley, A., Joy, K., Hunter, L., Tey, W., Abrahams, I., and Gerrish, L. 2020. The Spatial Flux of Earth's Meteorite Falls Found via Antarctic Data. *Geology* 48: 683–7.
Gattacceca, J., Valenzuela, M., Uehara, M., Jull, A. J. T., Giscard, M., Rochette, P., Braucher, R. et al. 2011. The Densest Meteorite Collection Area in Hot Deserts: The San Juan Meteorite Field (Atacama Desert, Chile). *Meteoritics & Planetary Science* 46: 1276–87.
Gnos, E., Lorenzetti, S., Eugster, O., Jull, A. J. T., Hofmann, B. A., Al-Khatiri, A., and Eggimann, M. 2009. The Jiddat al Harasis 073 Strewn Field, Sultanate of Oman. *Meteoritics & Planetary Science* 44: 375–87.
Halliday, I., Blackwell, A. T., and Griffin, A. A. 1989. The Flux of Meteorites on the Earth's Surface. *Meteoritics* 24: 173–8.
Halliday, I., Griffin, A. A., and Blackwell, A. T. 1996. Detailed Data for 259 Fireballs from the Canadian Camera Network and Inferences Concerning the Influx of Large Meteoroids. *Meteoritics & Planetary Science* 31: 185–217.
He, Q., Yang, X. H., Huo, W., Wang, S. G., Shang, K. Z., and Liu, H. Y. 2009. The Characteristics of Grain Size from the Kumtag Desert and its Environmental Significance. *Sciences in Cold and Arid Regions* 1: 128–34.
Hezel, D. C., Palme, H., Nasdala, L., and Brenker, F. E. 2006. Origin of SiO_2-Rich Components in Ordinary Chondrites. *Geochimica et Cosmochimica Acta* 70: 1548–64.
Hezel, D. C., SchlÜTer, J., Kallweit, H., Jull, A. J. T., Al, F. O., and Y., Al, Shamsi M., and Strekopytov, S. 2011. Meteorites from the United Arab Emirates: Description, Weathering, and Terrestrial Ages. *Meteoritics & Planetary Science* 46: 327–36.
Hofmann, B. A., Gnos, E., Jull, A. J. T., Szidat, S., Majoub, A., Al, W. K., Habibullah, S. N. et al. 2018. Meteorite Reconnaissance in Saudi Arabia. *Meteoritics & Planetary Science* 53: 2372–94.
Howie, R. M., Paxman, J., Bland, P. A., Towner, M. C., Cupak, M., Sansom, E. K., and Devillepoix, H. A. 2017. How to Build a Continental Scale Fireball Camera Network. *Experimental Astronomy* 43: 237–66.
Hu, F., and Yang, X. 2016. Geochemical and Geomorphological Evidence for the Provenance of Aeolian Deposits in the Badain Jaran Desert, Northwestern China. *Quaternary Science Reviews* 131: 179–92.
Hughes, D. W. 1992. The Meteorite Flux. *Space Science Reviews* 61: 275–99.
Hutchison, R. 2007. *Meteorites: A Petrologic, Chemical and Isotopic Synthesis*. Cambridge, UK: Cambridge University Press.
Hutson, M., Ruzicka, A., Timothy Jull, A. J, Smaller, J. E., and Brown, R. 2013. Stones from Mohave County, Arizona: Multiple Falls in the "Franconia Strewn Field". *Meteoritics & Planetary Science* 48: 365–89.
Hutzler, A., Gattacceca, J., Rochette, P., Braucher, R., Carro, B., Christensen, E. J., Cournede, C. et al. 2016. Description of a Very Dense Meteorite Collection Area in Western Atacama: Insight into the Long-Term Composition of the Meteorite Flux to Earth. *Meteoritics & Planetary Science* 51: 468–82.
Jull, A. J. T. 2006. Terrestrial Ages of Meteorites. In *Meteorites and the Early Solar System II*, edited by D. S. Lauretta and H. Y. McSween Jr., 889–905. Tucson, Arizona: The University of Arizona Press.
Jull, A. J. T., Cielaszyk, E., Cloudt, S. 1998. ^{14}C Terrestrial Ages of Meteorites from Victoria Land, Antarctica and the Infall Rates of Meteorites. In *Meteorites: Flux with Time and Impact Effects*, edited by M. M. Grady, R. Hutchison, G. J. H. McCall and D. A. Rothery. Geological Society of London Special Publication 140: 75–91.
Kring, D., Jull, A., McHargue, L., Bland, P., Hill, D., and Berry, F. 2001. Gold Basin Meteorite Strewn Field, Mojave Desert, Northwestern Arizona: Relic of a Small Late Pleistocene Impact Event. *Meteoritics & Planetary Science* 36: 1057–66.
Lewis, J. A., and Jones, R. H. 2019. Primary Feldspar in the Semarkona LL 3.00 Chondrite: Constraints on Chondrule

Formation and Secondary Alteration. *Meteoritics & Planetary Science* 54: 72–89.
Li, J., Dong, Z., Qian, G., Zhang, Z., Luo, W., Lu, J., and Wang, M. 2016. Yardangs in the Qaidam Basin, Northwestern China: Distribution and Morphology. *Aeolian Research* 20: 89–99.
Li, J., Wen, S., Zhang, Q., Wang, F., Zheng, B., and Li, B. 1979. The Time, Magnitude and Modes of Uplift of the Qinghai-Tibetan Plateau. *Science in China (Series A)* 6: 608–16 (in Chinese).
Li, S. L., and Hsu, W. B. 2014. New Dense Meteorite Collection Areas Were Found in Lop Nur, Xinjiang. *Chinese Science Bulletin* 59: 2091–7 (in Chinese).
Li, S. J., Leya, I., Wang, S. J., Smith, T., Bao, H. M., Fan, Y., and Mo, B. 2021. Exposure History, Petrology, and Shock Induced Vulcanization Reaction of Alatage Mountain 001 Strewn Field Samples. *Meteoritics & Planetary Science* 56: 1293–310.
Li, S. J., Wang, S. J., Leya, I., Smith, T., Tang, J. L., Wang, P., Zeng, X. J., and Li, Y. 2017. A Chondrite Strewn Field Was Found in East of Lop Nor, Xinjiang. *Chinese Science Bulletin* 62: 2407–15 (in Chinese).
Liu, Z. C., Wang, Y. J., Chen, Y., Li, X. S., and Li, Q. C. 1998. Magnetostratigraphy and Sedimentologically Derived Geochronology of the Quaternary Lacustrine Deposits of a 3000 m Thick Sequence in the Central Qaidam Basin, Western China. *Palaeogeography, Palaeoclimatology, Palaeoecology* 140: 459–73.
Lu, Q., Wu, B., Dong, Z. B., Lu, H. Y., Xiao, H. L., and Wang, J. H. 2012. *A Study of the Kumtag Desert*. Beijing: Science Press.
Muñoz, C., Guerra, N., Martínez-Frías, J., Lunar, R., and Cerda, J. 2007. The Atacama Desert: A Preferential Arid Region for the Recovery of Meteorites—Find Location Features and Strewnfield Distribution Patterns. *Journal of Arid Environments* 71: 188–200.
Nazarov, M. A., Badyukov, D. D., Lorents, K. A., and Demidova, S. I. 2004. The Flux of Lunar Meteorites onto the Earth. *Solar System Research* 38: 49–58.
Nishiizumi, K., Okazaki, R., Park, J., Nagao, K., Masarik, J., and Finkel, R. 2002. Exposure and Terrestrial History of Dhofar 019 Martian Meteorite (Abstract #1366). 33rd Lunar and Planetary Science Conference. CD-ROM.
Ouazaa, N. L., Perchiazzi, N., Kassaa, S., Zeoli, A., Ghanmim, M., and Folco, L. 2009. Meteorite Finds from Southern Tunisia. *Meteoritics & Planetary Science* 44: 955–60.
Ouknine, L., Khiri, F., Ibhi, A., Heikal, M. T. S., Saint-Gerant, T., and Medjkane, M. 2019. Insight into African Meteorite Finds: Typology, Mass Distribution and Weathering Process. *Journal of African Earth Sciences* 158: 103551.
Pourkhorsandi, H., D'Orazio, M., Rochette, P., Valenzuela, M., Gattacceca, J., Mirnejad, H., Sutter, B., Hutzler, A., and Aboulahris, M. 2017. Modification of REE Distribution of Ordinary Chondrites from Atacama (Chile) and Lut (Iran) Hot Deserts: Insights into the Chemical Weathering of Meteorites. *Meteoritics & Planetary Science* 52: 1843–58.
Pourkhorsandi, H., Gattacceca, J., Rochette, P., D'Orazio, M., Kamali, H., Avillez, R., Letichevsky, S. et al. 2019. Meteorites from the Lut Desert (Iran). *Meteoritics & Planetary Science* 54: 1737–63.
Qian, G., Yang, Z., Luo, W., Dong, Z., Lu, J., and Tian, M. 2020. Morphological and Sedimentary Characteristics of Dome Dunes in the Northeastern Qaidam Basin, China. *Geomorphology* 350: 106923.
Qu, J. J., Liao, K. T., Zu, R. P., Xia, X. C., Jing, Z. F., Dong, Z. B., Zhang, K. C., Yang, G. S., Wang, X. M., and Dong, G. R. 2007. Study on Formation Mechanism of Feather-Shaped Sand Ridge in Kumtag Desert. *Journal of Desert Research* 27: 349–53 (in Chinese).
Rieser, A. B., Neubauer, F., Liu, Y., and Ge, X. 2005. Sandstone Provenance of North-Western Sectors of the Intracontinental Cenozoic Qaidam Basin, Western China: Tectonic vs. Climatic Control. *Sedimentary Geology* 177: 1–18.
Rubin, A. E., and Read, W. F. 1984. The Brownell and Ness County (1894) L6 Chondrites: Further Sorting-Out of Ness County Meteorites. *Meteoritics* 19: 153–60.
Rubin, A. E., Verish, R. S., Moore, C. B., and Oriti, R. A. 2000. Numerous Unpaired Meteorites Exposed on a Deflating Playa Lake at Lucerne Valley, California. *Meteoritics & Planetary Science* 35: A181–3.
Schlüter, J., Schultz, L., Thiedig, F., Al-Mahdi, B. O., and Abu, A. E. 2002. The Dar al Gani Meteorite Field (Libyan Sahara): Geological Setting, Pairing of Meteorites, and Recovery Density. *Meteoritics* 37: 1079–93.
Shen, Y. C., Wang, X. H., Cheng, W. M., Wu, J. F., Lu, Q., and Feng, Y. M. 2016. Integrated Physical Regionalization of Stony Deserts in China. *Progress in Geography* 35: 57–66 (in Chinese).
Van Schmus, W. R., and Wood, J. A. 1967. A Chemical-Petrologic Classification for the Chondritic Meteorites. *Geochimica et Cosmochimica Acta* 81: 747–65.
Vickery, A. M., and Melosh, H. J. 1987. The Large Crater Origin of SNC Meteorites. *Science* 237: 738–43.
Wang, F., Sun, D., Chen, F., Bloemendal, J., Guo, F., Li, Z., Zhang, Y., Li, B., and Wang, X. 2015. Formation and Evolution of the Badain Jaran Desert, North China, As Revealed by a Drill Core from the Desert Centre and by Geological Survey. *Palaeogeography, Palaeoclimatology, Palaeoecology* 426: 139–58.
Wei, H. D., Xu, X. Y., Wang, J. H., Tang, J. N., Liu, H. J., Ding, F., Liao, K. T. et al. 2007. Analysis of Grain Size of Different Sand Dunes Types in Kumtag Desert. *Journal of Soil and Water Conservation* 21: 6–9 (in Chinese).
Weisberg, M. K., Smith, C., Benedix, G., Herd, C. D. K., Righter, K., Haack, H., Yamaguchi, A., Chennaoui, A. H., and Grossman, J. N. 2010. The Meteoritical Bulletin, No. 97. *Meteoritics & Planetary Science* 45: 449–93.
Wlotzka, F. 1993. A Weathering Scale for the Ordinary Chondrites. *Meteoritics* 28: 460.
Xia, W. C., Zhang, N., Yuan, X. P., Fan, L. S., and Zhang, B. S. 2001. Cenozoic Qaidam Basin, China: A Stronger Tectonic Inversed, Extensional Rifted Basin. *AAPG Bulletin* 85: 715–36.
Yang, X., Ma, N., Dong, J., Zhu, B., Xu, B., Ma, Z., and Liu, J. 2010. Recharge to the Inter-Dune Lakes and Holocene Climatic Changes in the Badain Jaran Desert, Western China. *Quaternary Research* 73: 10–9.
Ye, C., Yang, Y., Fang, X., and Zhang, W. 2016. Late Eocene Clay Boron-Derived Paleosalinity in the Qaidam Basin and its Implications for Regional Tectonics and Climate. *Sedimentary Geology* 346: 49–59.
You-hao, E., Su, Z. Z., Wang, J. H., Zhai, X. W., Liu, H. J., Tang, J. N., Ding, F., Zhang, J. C., Liao, K. T., and

Zheng, Q. Z. 2006. Outcome and Scientific Significance of Integrated Investigation in Kumtag Desert. *Journal of Desert Research* 26: 693–7 (in Chinese).
Zeng, X. J., Li, S. J., Leya, I., Wang, S. J., Smith, T., Li, Y., and Wang, P. 2018. The Kumtag 016 L5 Strewn Field, Xinjiang Province, China. *Meteoritics & Planetary Science* 53: 1113–30.
Zhang, Y. and Xuan, Z. 1996. Economic Evaluation of Potassium and Magnesium Solid Deposit in Kunteyi and Mahai Salt Lake of Qinghai Province. *Journal of Salt Lake Science* 4: 36–45 (in Chinese).
Zhang, Z., Dong, Z., and Li, C. 2015. Wind Regime and Sand Transport in China's Badain Jaran Desert. *Aeolian Research* 17: 1–13.
Zhong, D. C. 2003. *Dynamical Change Map of Modern Sand Desert in China (1:4,000000)*. Beijing: Sinomap Press.
Zolensky, M., Bland, P., Brown, P., and Halliday, I. 2006. Flux of Extraterrestrial Materials. In *Meteorites and the Early Solar System II*, edited by D. S. Lauretta and H. Y. McSween Jr., 869–88. Tucson, Arizona: The University of Arizona Press.
Zolensky, M. E., Schutt, J. W., Reid, A. M., Jakeš, P., de Los, Martinez, Rios, E., and Miller, R. M. 1995. Locating New Meteorite Recovery Areas. Workshop on the Extraterrestrial Materials from Cold and Hot Desert Areas. pp. 78–80.
Zolensky, M. E., Wells, G. L., and Rendell, H. M. 1990. The Accumulation Rate of Meteorite Falls at the Earth's Surface: The View from Roosevelt County, New Mexico. *Meteoritics* 25: 11–7.
Zurfluh, F. J., Hofmann, B. A., Gnos, E., Eggenberger, U., and Jull, A. J. T. 2016. Weathering of Ordinary Chondrites from Oman: Correlation of Weathering Parameters with ^{14}C Terrestrial Ages and a Refined Weathering Scale. *Meteoritics & Planetary Science* 51: 1685–700.

SUPPORTING INFORMATION

Additional supporting information may be found in the online version of this article.

Data S1. Additional backscattered electron (BSE) images.

Data S2. Additional photographs for the studied ordinary chondrites.

Table S1. The original data of mineral compositions of the studied 49 ordinary chondrites.

Table S2. The coordinates, mass, piece, and main mass location of the studied meteorites.